Modelling of plankton and forage fish variability in the Gulf of Kachchh using 2D coupled physico-biological model

Vijay Kumar[1,*], Girija Jayaraman[1,2] and Beena Kumari[3]

[1]Indian Institute of Technology Delhi, Hauz Khas, New Delhi 110 016, India
[2]The University of the West Indies, Mona, Kingston, Jamaica, West Indies
[3]Space Applications Centre, Indian Space Research Organisation, Ahmedabad 380 015, India

A biophysical coupled model, which includes interaction of processes at different spatial and temporal scales, is used to assess the seasonal variability of plankton and forage fish. A five-compartment nutrient, phytoplankton, zooplankton, detritus, forage (NPZDF) ecological model is coupled with hydrodynamic model to understand the interaction of hydrographic characteristics and ecological dynamics in the study area. Operator splitting method is used to handle two different physical and biological scales for numerical simulation of the resulting partial differential equations. Gulf of Kachchh (22°20′N–23°40′N, 68°20′E–70°40′E), in the northwest coast of India is used for the application and validation of the model's behaviour. This region demonstrates rich biodiversity and productivity in highly turbid and varying marine conditions. Co-ordinate transformation is used to convert the irregular coastal geometry of Gulf of Kachchh into a rectangular domain. Numerical experiments, together with sensitivity analysis are carried out to get the values/ranges of the model parameters. The model application is able to bring out many striking features of the Gulf of Kachchh including bimodal oscillations observed in the ecological data of the region.

Keywords: Gulf of Kachchh, physico-biological model, plankton and forage fish.

ECOSYSTEM models for marine species are based on an ecosystem management approach and species by species analytical stock assessment using population dynamics. Food is an important factor that influences growth, migration and abundance of fish stock both in time and space[1]. Light and circulation are the major physical factors and nutrient and plankton constitute the major biological factors for selecting their habitat and growth by species in the marine environment.

Plankton production in aquatic environment depends upon availability of nutrient and light. A basic mathematical formulation for nutrient and plankton dynamics has been reported earlier[2–4]. Nutrients are dissolved inorganic forms of nitrogen, phosphorus and silicon, which are utilized by photosynthetic organisms in the formation of organic matter or phytoplankton. Phytoplanktons are plant forms of plankton community, capable of photosynthesis in the presence of sunlight and serve as the basic food source for all aquatic food chain. Zooplanktons are small floating animals and are predators of phytoplankton. Along with phytoplankton, they make up the planktonic food supply in food chain. Forage fish production is based on ecological transfer of primary production to forage. It is a secondary consumer and occupies central position in the marine food web. Higher concentration of primary production conserves alleviated level of secondary and tertiary production. This process of forage fish production has been modelled earlier[5,6] where a model of tuna forage distribution in the equatorial pacific based on advection–diffusion reaction equation was proposed with constant recruitment of primary production.

The physical, biological and chemical processes are usually represented by a system of partial differential equations in a mathematical framework referred to as the system of advection–diffusion-reaction equations. The advection and diffusion terms represent physical processes while the reaction term in the governing equations represent biological and chemical processes. Due to their highly nonlinear nature and different temporal scales, the governing equations together with boundary conditions form a stiff boundary value problem of evolution type. Such problems are difficult to solve and a common approach employed is an operator splitting technique (OST) followed by an accurate numerical scheme. The method consists of decomposing the problem into components where each component problem corresponds to a characteristic scale of a physical or biological process. OST thus transforms a complex problem into a sequence of simpler tasks. Finally, a global solution is sought by iterating the solution of different components. It is second-order accurate[7,8]. For example, it is appropriate to elaborate how OST has been applied for the advection–diffusion-reaction equation which embodies two time scales: (i) a relatively faster time scale concerning advection–diffusion phenomen and (ii) a grossly slow time

*For correspondence. (e-mail: vijayiitdelhi@gmail.com)

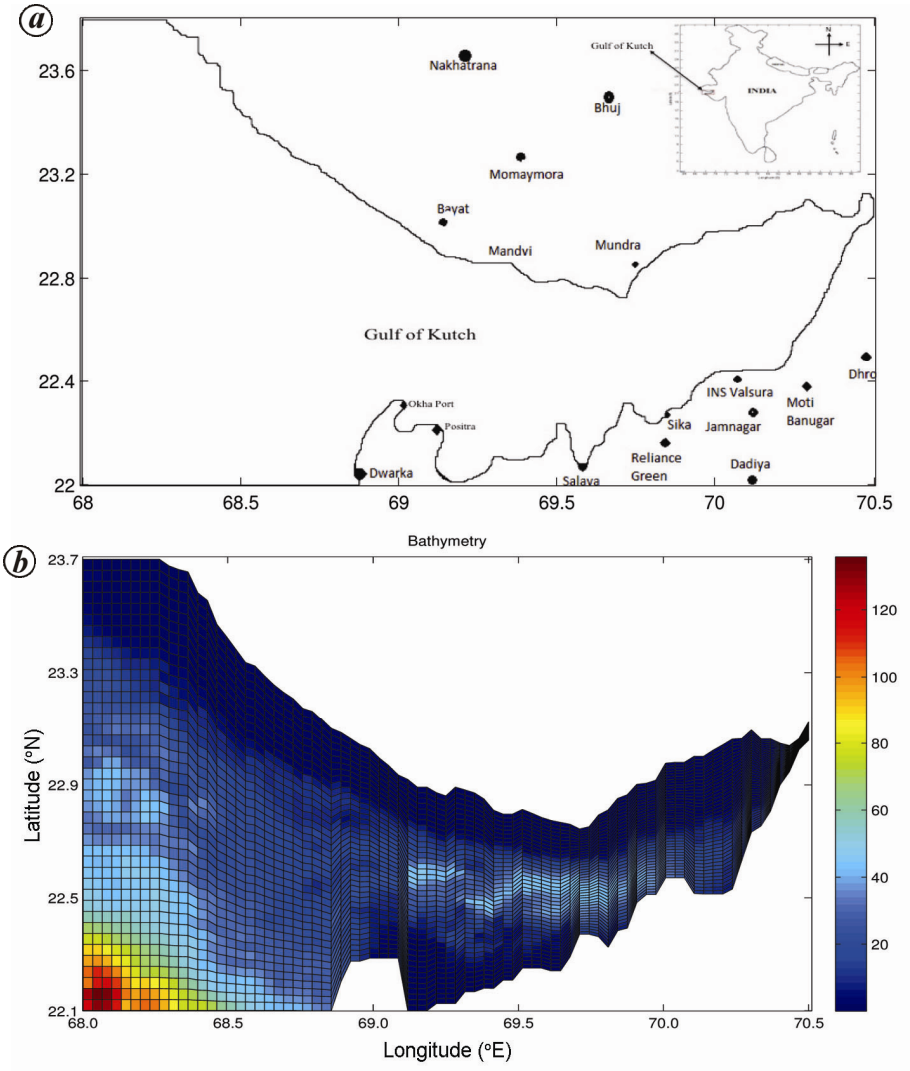

Figure 1. Plot of study area and bathymetry. ***a***, Gulf of Kachchh of study area. ***b***, Bathymetry (m) (http://apdrc.soest. hawaii.edu/las/v6/constrain?var=325).

scale for biological and chemical reactions in the system. The problem is therefore split into two and a solution for a single time step is accomplished in two stages: the first stage involves solution of the non-reactive (or without source) component problem represented by advection–diffusion type equation; and the final stage is completed by obtaining the solution of reactive equations (or with source)[9]. Advection–diffusion equations are usually solved with a finite difference or finite element methods, while reactive equations are normally solved with an ordinary differential equations integrator. Wheeler and Dawson[9] used a time splitting algorithm for solving a system of two-dimensional nonlinear advection–diffusion-reaction equations.

The main objective of this article is to reproduce the spatial-temporal distribution of nutrient, plankton and forage fish in Gulf of Kachchh. A coordinate transformation is used to convert the physical domain into a rectangular domain so that a second order finite difference numerical technique could be used. This model might be of interest to ecological modellers, as it enables to bring out the essential features of the data like the bimodal oscillations in the monthly mean chlorophyll-*a* of SeaWiFs data.

Study area

Gulf of Kachchh (22°20′N–23°40′N, 68°20′E–70°40′E) is an inlet of the Arabian Sea, west coast of India, in Jamnagar district of Gujarat state (Figure 1 *a*). It is a shallow water body with depth extending from 120 m at the mouth to less than 20 m at the head (Figure 1 *b*). The climate is semi-arid and the maximum rainfall is 50 cm/year. It has little run-off from land and no major river flows into it. However, a large volume of suspended

Table 1. Observed data at the Kandla Creek of Gulf of Kachchh[11]

Variable	Range	Minimum	Maximum	Average	Standard
Pre-monsoon (February–May)					
Nutrient (µmol N/l)	91.5	4.9	96.4	38.0	5.34
Chlorophyll *a* (mg/m^3)	2.4	0.2	2.6	0.9	0.6
Primary production (mg/m^{3}h)	1.7	0.0	1.7	0.5	0.6
Monsoon (June–September)					
Nutrient (µmol N/l)	72.1	12.3	84.4	40.5	4.06
Chlorophyll *a* (mg/m^3)	1.8	0.1	1.9	0.6	0.4
Primary production (mg/m^{3}h)	1.2	0.1	1.3	0.5	0.5
Post-monsoon (October–January)					
Nutrient (µmol N/l)	79.5	10.0	89.5	42.4	4.68
Chlorophyll *a* (mg/m^3)	2.0	0.1	2.1	0.7	0.6
Primary production (mg/m^{3}h)	1.9	0.0	1.9	0.7	0.7

sediments enters into the Gulf from northwestern side. Moreover, low turbid water masses from south travel northwards along the southeastern coast and finally move towards the northeast[10]. Most importantly, Gulf of Kachchh is one of the few coastal zones in the world that has rich bio-diversity and high productivity.

Nutrient and plankton characteristics of the study area

Sediments and dust particles transported by eddies during post-monsoon season in the water column of Gulf of Kachchh, remineralize to nutrients that, in turn, lead to an abundance of nutrients. Sufficient light helps in more phytoplankton growth. During winter, light for photosynthesis is insufficient, hence phytoplankton growth rate decreases. However, dead plant biomass and organic matter also remineralize to nutrients during spring season, thus making them abundant. Higher concentrations of phytoplankton increase zooplankton growth and forage fish reach its maximum during spring and post-monsoon. Average catch of fish is 1.4×10^5 tonnes/year. Thus, Gulf of Kachchh provides suitable ecological and environmental conditions for marine species (http://www.icmam.gov.in/GOK.PDF).

Table 1 (ref. 11) gives an average of five years data, based on the observations for nutrients (phosphate, nitrate, nitrite, ammonia and silicate) and phytoplankton at the Kandla Creek (22°55′N–23°05′N, 70°20′E–70°40′E) during 2002 to 2006. Water samples were collected regularly twice in every season; pre-monsoon (February–May), monsoon (June–September) and post-monsoon (October–January) during five years. The concentrations of nutrient, chlorophyll-*a* and primary production and the ranges of their variation are more during pre- and post-monsoon than those during monsoon for all the observed data.

Figure 2 *a–c* is based on the monthly time series of plankton data[12] at the Okha port during 1969. Cubic spline is used for interpolation. Two peaks are seen for phytoplankton (Figure 2 *a*), a primary one in September–October due to a bloom and secondary peak in January or June due to more than one genus and species of diatoms. More than one peak is observed for zooplankton (Figure 2 *b*), a primary peak in October and a secondary peak in March, though a minimum is observed in August. The time lag between phytoplankton and zooplankton bloom is around 30 days (Figure 2 *c*). *In situ* measurement in Table 1 shows maximum concentration of nutrient, chlorophyll-*a* and primary production during peak period in Figure 2.

Figure 3 shows SeaWiFs estimated monthly mean area of averaged chlorophyll-*a* and interpolated data of 2010 along with a continuous curve for the study area (68°E–70°E, 22°N–23°N). The bimodal distributions show two peaks, a major during September and a minor in April.

The entire plankton data (Table 1, Figures 3 and 4) show two peaks in the monthly data of a year, i.e. one minor in spring season and one major in post-monsoon. This is because spring and post-monsoon periods have sufficient light and nutrient to increase both phytoplankton and zooplankton production.

Ocean currents in the study area (selected grids)

Limited data on ocean currents ($0.5° \times 0.5°$ grid size) is available on the website http://las.incois.gov.in/las/UI.vm. In this study, coarser current field of 2010 has been interpolated to a finer field using the method of cubic splines. The interpolated field for the whole domain at a resolution of $0.05° \times 0.05°$ is finer than the minimum phytoplankton patch of about 22 km size as shown in Figure 4 (ref. 1). The region has seasonally reversing monsoonal currents forced by monsoonal winds that dominate the physical processes. The summer monsoonal current (SMC) flows eastward during summer monsoon (May–September) and the winter monsoon current (WMC) flows westward during the winter monsoon

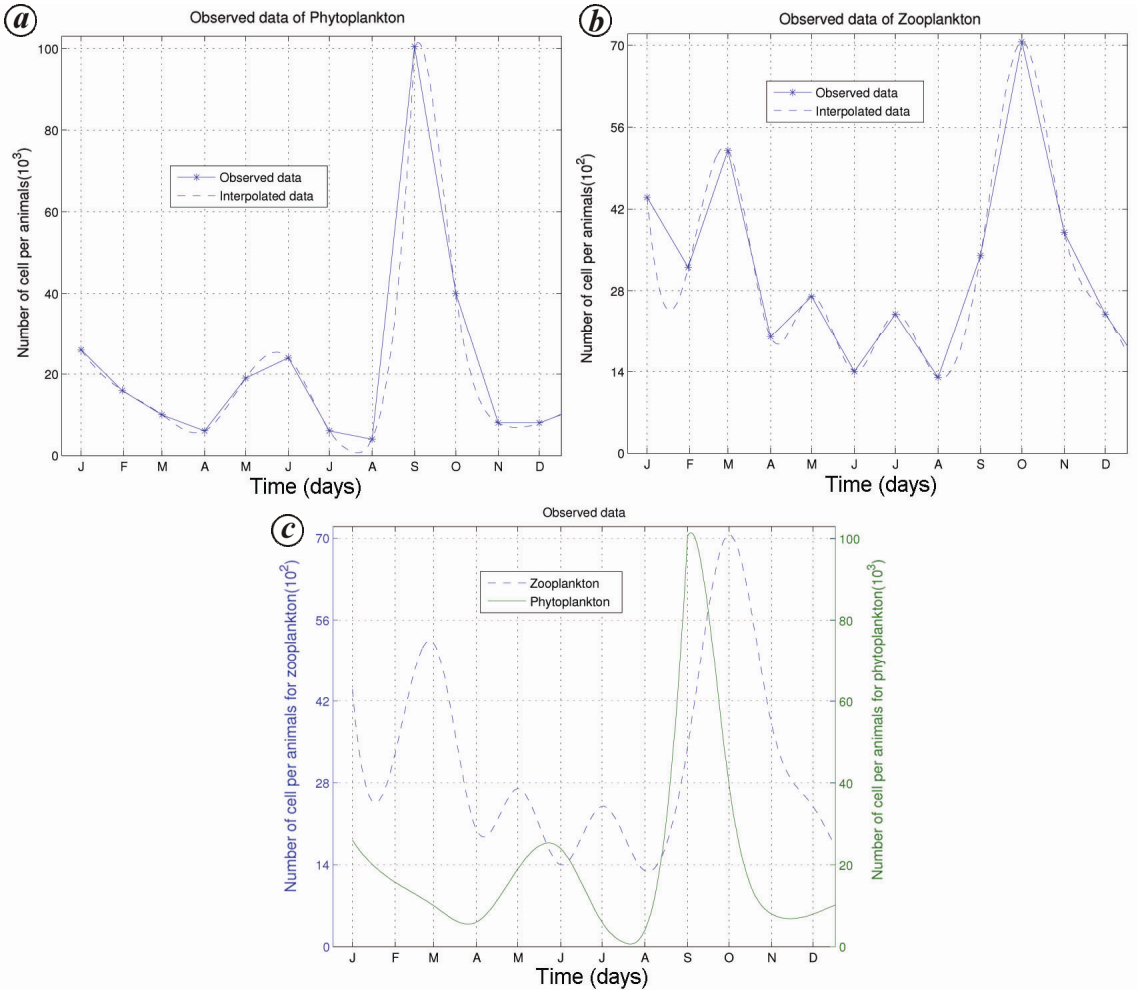

Figure 2. Plots of observed (-*-) and interpolated (-) data[12]. ***a***, Phytoplankton; ***b***, Zooplankton; ***c***, Interpolated phytoplankton and zooplankton.

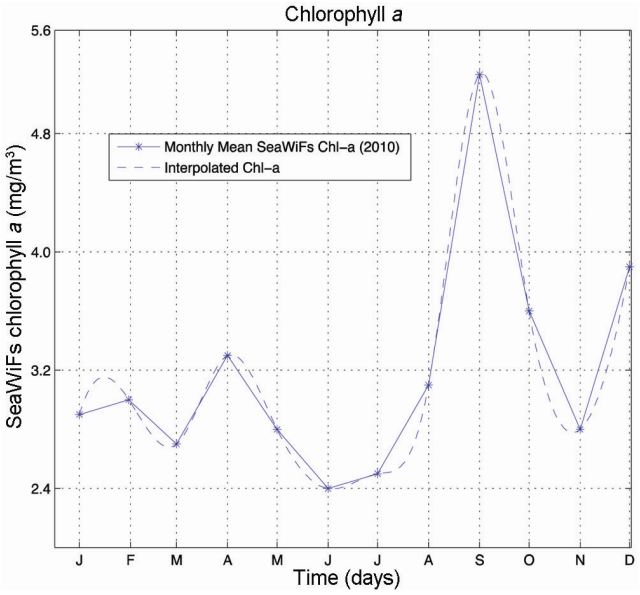

Figure 3. Area averaged interpolated and monthly mean SeaWiFs Chl *a*, 2010.

(November–February)[13]. Figure 4 shows the flow of ocean currents, northeast in May–August and southwest in November–February. The seasonally reversing wind driven circulation is responsible for the upward movement of nutrients from the bottom to top layer in a water column which impacts the marine biological processes in the region.

Model structure and equations

Compartmental ecosystem models of the mixed layer are widely used in marine ecology. The coupling of different compartments is the key issue in mathematical modelling as different compartments represent phenomena that have different time scales. In this regard, Steele[14] and Fasham *et al.*[3] made a basic assumption that the mixed layer could be considered biologically homogeneous. Therefore, one may assume that the physical mixing rates in the biological homogeneous layer are faster compared to the growth rates of organisms. This simplification has

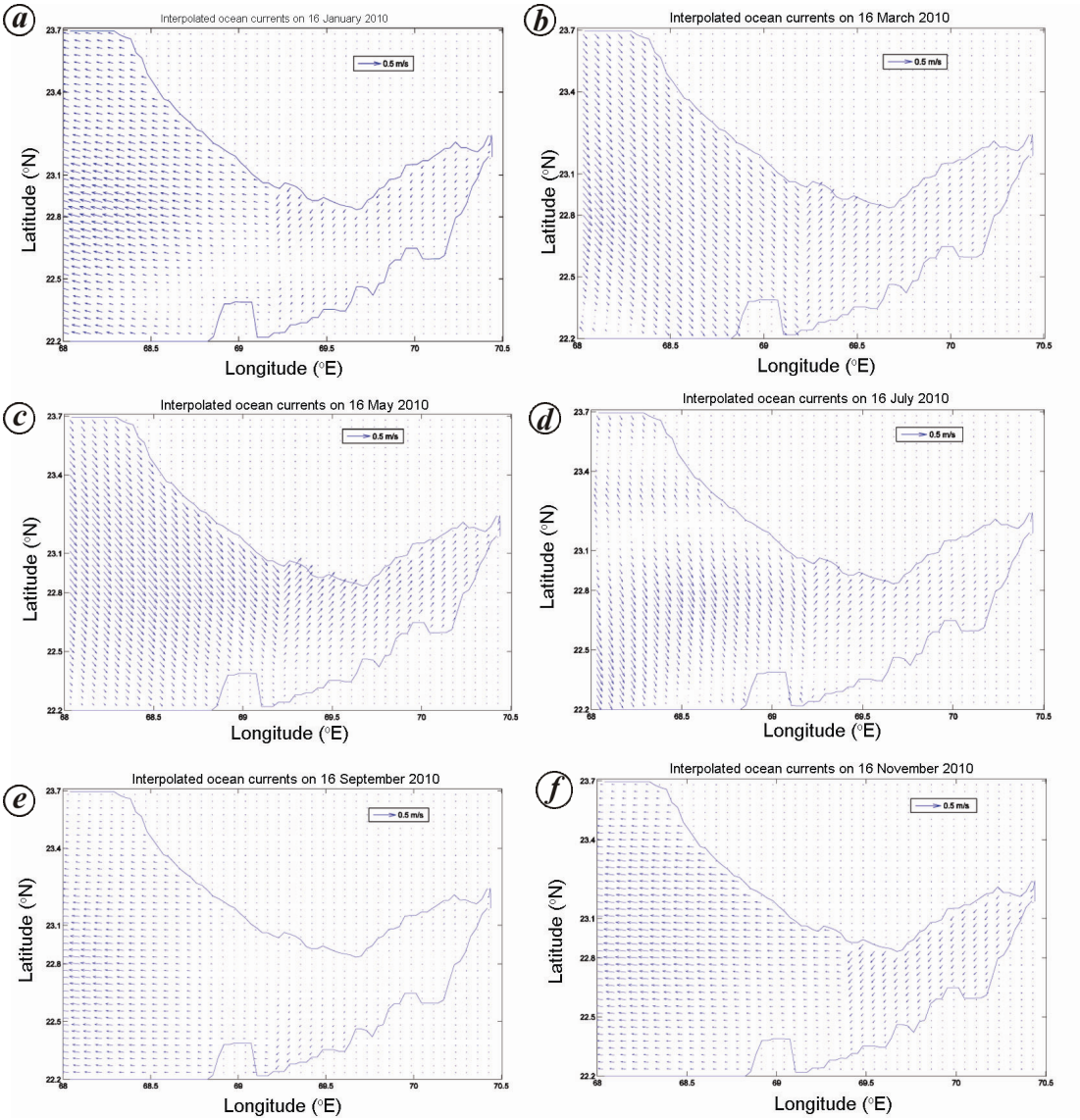

Figure 4. Plots of ocean currents from interpolated data. ***a***, 16 January 2010; ***b***, 16 March 2010; ***c***, 16 May 2010; ***d***, 16 July 2010; ***e***, 16 September 2010; ***f***, 16 November 2010.

probably proved to be a robust assumption in most cases of ocean basin and hence it has also been applied in the model formulation of this study. Further, ecosystem seasonality has been assumed to be driven by seasonal changes in incident photosynthetically active radiation (PAR) and vertical depth of coastal basin[3]. The formulation of biological model is similar to those used in earlier studies[2,6,15,16]. The governing equations of the two-dimensional physical-biological model for the five compartments are described in the following section.

Governing equations

$$\frac{\partial N}{\partial t}+u\frac{\partial N}{\partial x}+v\frac{\partial N}{\partial y}=\sigma_x\frac{\partial^2 N}{\partial x^2}+\sigma_y\frac{\partial^2 N}{\partial y^2}+B_N, \quad (1)$$

$$\frac{\partial P}{\partial t}+u\frac{\partial P}{\partial x}+v\frac{\partial P}{\partial y}=\sigma_x\frac{\partial^2 P}{\partial x^2}+\sigma_y\frac{\partial^2 P}{\partial y^2}+B_P, \quad (2)$$

$$\frac{\partial Z}{\partial t}+u\frac{\partial Z}{\partial x}+v\frac{\partial Z}{\partial y}=\sigma_x\frac{\partial^2 Z}{\partial x^2}+\sigma_y\frac{\partial^2 Z}{\partial y^2}+B_Z, \quad (3)$$

$$\frac{\partial D}{\partial t}+u\frac{\partial D}{\partial x}+v\frac{\partial D}{\partial y}=\sigma_x\frac{\partial^2 D}{\partial x^2}+\sigma_y\frac{\partial^2 D}{\partial y^2}+B_D, \quad (4)$$

$$\frac{\partial F}{\partial t}+u\frac{\partial F}{\partial x}+v\frac{\partial F}{\partial y}=\sigma_x\frac{\partial^2 F}{\partial x^2}+\sigma_y\frac{\partial^2 F}{\partial y^2}+B_F, \quad (5)$$

where

$$B_N = -\left\{\frac{\alpha(\phi,H,t)N}{K_N+N} - r\right\}P + r_1 D + \frac{m_0}{H}(N_S - N), \quad (6)$$

$$B_P = \left\{\frac{\alpha(\phi,H,t)N}{K_N+N} - r\right\}P - \frac{p_1 P}{A}\frac{c(A-A_{th})Z}{K_Z+(A-A_{th})} - \frac{\mu P^2}{K_P+P} - \frac{m_0}{H}P, \quad (7)$$

$$B_Z = \frac{ec(A-A_{th})Z}{K_Z+(A-A_{th})} - gZ, \quad (8)$$

$$B_D = \frac{\mu P^2}{K_P+P} - r_1 D + \frac{p_1 P}{A}\frac{(1-e)c(A-A_{th})Z}{K_Z+(A-A_{th})} - \frac{p_2 D}{A}\frac{ec(A-A_{th})Z}{K_Z+(A-A_{th})}, \quad (9)$$

$$B_F = -\lambda F + e^{m_r t_r} PP, \quad (10)$$

$$N_S = 10\left(1+\cos\left(\frac{4\pi}{365}(284+t)\right)\right),$$

$$A = p_1 P + p_2 D \text{ and } m_r = -\log\left(\frac{0.04}{t_r}\right). \quad (11)$$

The parameters and different terms have been explained in detail in the section description of the terms of the ecological model. More information could be obtained from the refs 2, 3, 6, 15 and 16.

Initial and boundary conditions

Equations (1)–(5) are of evolution-type and involve two space variables (x, y). Hence to resolve the governing set of equations, an initial distribution over the study domain and appropriate boundary conditions for each species are required to limit the numerical solution.

Initial conditions: Initial conditions are prescribed by assigning a constant value to each variable which evolve in course of time as the model integration proceeds. Thus, we have at $t = 0$.

$$N(x,y,0) = N_0,\ P(x,y,0) = P_0,\ Z(x,y,0) = Z_0,$$

$$D(x,y,0) = D_0 \text{ and } F(x,y,0) = F_0, \quad (12)$$

where N_0, P_0, Z_0, D_0 and F_0 are constant values of the dependent variables at $t = 0$. Since the equations are of evolution type, if their integration is carried out sufficiently long, the system will reach a steady state which would be independent of the prescribed initial conditions but would depend on the boundary conditions though.

Boundary conditions: Along the coastline, diffusive flux of all biological tracers is assumed to vanish, that is

$$\frac{\partial N}{\partial \eta} = \frac{\partial P}{\partial \eta} = \frac{\partial Z}{\partial \eta} = \frac{\partial D}{\partial \eta} = \frac{\partial F}{\partial \eta} = 0 \frac{\partial B}{\partial \eta} = 0,$$

at the coastal boundary, (13)

where η is a unit vector perpendicular to the coastline. On the open ocean side, concentrations of the biological tracers are prescribed as

$$N = N_b,\ P = P_b,\ Z = Z_b,\ D = D_b \text{ and } F = F_b,$$

along the open ocean boundary. (14)

The values of N_b, P_b, Z_b, D_b and F_b at the boundary are given in Table A1 of Appendix A.

Description of the terms of the ecological model

The terms on the left side of eqs (1)–(5) represent the rate of change of the respective biological tracer and the horizontal advection by ocean currents. Zonal and meridional components are given by u and v respectively. The velocity field (u, v) has been taken from the ocean circulation model (http://www.incois.gov.in/Incois/indofos_surface-currents.jsp). The terms on the right side represent the diffusion and source terms of biological tracers (N, P, Z, D, F). The diffusion coefficients $\sigma_x = \sigma_y = \sigma$ are taken as a constant and their values prescribed within the range lying between 100 m^2/s and 3200 m^2/s (ref. 17).

Nutrients (N): Equation (1) represents the mathematical expression of temporal and spatial distribution of nutrient. $-\{(\alpha(\phi,H,t)N)/(K_N+N)\}P$ represents the loss due to the uptake of nutrient by phytoplankton and rp represents the recruitment due to metabolic loss of phytoplankton. $\{(\alpha(\phi,H,t)N)/(K_N+N)\}$ is the average daily phytoplankton specific growth rate according to Michaelis–Menten hyperbola where $\alpha(\phi, H, t)$ is the light limited growth rate and $\{N/(K_N+N)\}$ is a non-dimensional nutrient limiting factor. $\alpha(\phi, H, t)$ is also called photosynthetic rate of phytoplankton[2] which changes periodically over a period of one year (Figure 5). In order to implement annual changes of temperature and light and also to incorporate the seasonal sequence of events, the formulation of Evans and Parslow[2] is followed accordingly

$$\alpha(\phi,H,t) = \frac{2Q}{k_1 H}\int_0^{\tau}\int_{\beta}^{\beta e^{k_1 H}} \frac{x\,dy\,dx}{y\sqrt{(y^2+x^2)}}, \quad (15)$$

where

$$\beta = \frac{Q\tau}{k_2 J}, \tau = \frac{1}{2}\cos^{-1}(-\tan\delta\tan\phi),$$

$$\delta = 23.45\sin(2\pi(284+\text{days})/365), \quad (16)$$

$$J = \frac{R}{\pi}(\tau\sin\delta\sin\phi + \cos\delta\cos\phi\sin\tau),\ R = \frac{3}{8}(1-a_0)S_0. \quad (17)$$

The term $r_1 D r_1 D$ corresponds to remineralization of detritus into nutrient, while $((m_0 + \zeta^+(t))/H)N_0$ represents addition of nutrient in the system through vertical diffusion from sediments at the depth H; N_S being the sediment nutrient concentration; and m_0 is the vertical mixing rate. The sediments in the Gulf of Kachchh are suspended matter and clay particles with high concentration between 21 mg/l and 69 mg/l (ref. 18).

Phytoplankton (P): Equation (2) represents the mathematical expression of temporal and spatial distribution of phytoplankton. There are several terms in this equation that pertain to different mechanisms: $-\mu P^2/(K_P + P)$ is the congestion mortality of phytoplankton

$$\frac{p_1 P}{A}\frac{c(A-A_{th})Z}{K_Z + (A-A_{th})}$$

represents the loss of phytoplankton due to grazing by zooplankton; and

$$-\frac{m_0 + \varsigma^+(t)}{H(t)}P$$

corresponds to the loss of phytoplankton to the bottom of shallow water body.

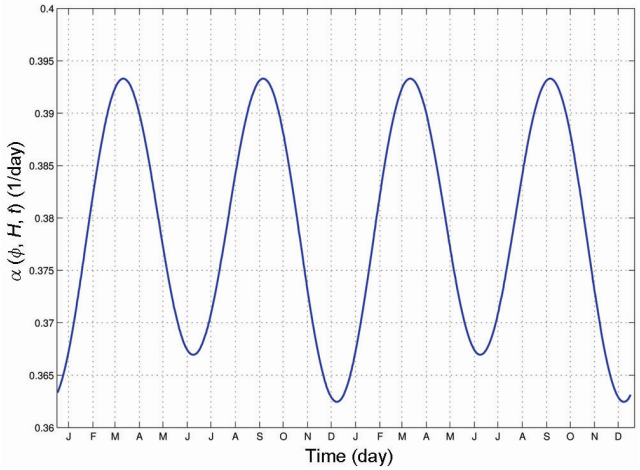

Figure 5. Photosynthetic rate of phytoplankton at (23°N, 69°54′E).

Zooplankton (Z): Equation (3) represents the mathematical expression of temporal and spacial distribution of zooplankton.

$$\frac{ec(A-A_{th})Z}{K_Z + (A-A_{th})},$$

is the growth term due to grazing of phytoplankton and detritus by zooplankton. The term $-gZ$ is the natural mortality.

Detritus (D): Detritus is a non-living particulate organic material. It includes the bodies or fragments of dead organisms as well as faecal material. Detritus is typically colonized by communities of microorganisms, which act to decompose (or remineralize) the material. It is assumed that detritus could be recycled within water column by two mechanisms, re-ingestion by zooplankton or remineralization of it into nutrient.

Equation (4) represents the mathematical expression of temporal and spatial distribution of detritus.

$$\frac{p_1 P}{A}\frac{(1-e)c(A-A_{th})Z}{K_Z + (A-A_{th})}$$

represents the growth term due to unassimilated phytoplankton and

$$\frac{p_2 D}{A}\frac{ec(A-A_{th})Z}{K_Z + (A-A_{th})}$$

is the loss term due to grazing of detritus by zooplankton.

Forage fish (F): Forage fish are small pelagic fish, which are preyed upon by larger predators. The ocean primary producers mainly contain planktons which produce food energy from the sun and forage fish transfer this energy by eating the planktons and in turn become food for the higher predators. Thus, forage fish occupy central position in the ocean food web.

Equation (5) represents temporal and spatial distribution of forage fish. λF is the total mortality (natural and fishing mortality) and $\exp(m_{rtr})PP$ represents the recruitment of forage fish in the form of primary production PP with unit mmol N/m^{3}day.

The parameters and their range of values listed in Table 2 are taken from literature[2,3,6,15,16,19] and sensitive analysis.

Numerical description

Equations (1)–(5) for advection–diffusion-reaction type equations are given by

$$\frac{\partial B}{\partial t} = \nabla(\sigma\nabla B) - V.\nabla B + f(\alpha, H, B, t), \quad (18)$$

Table 2. Description of parameters used in simulations

Parameter	Parameter description	Unit	Value and range
$\alpha(\phi, H, t)$	Light photosynthetic rate	1/day	–
H	Depth of shallow region of Ocean	m	–
t_r	Characteristic time of recruitment	day	100 (90–120)
K_N	Uptake half saturation	mmol N/m^3	0.5 (0.25–0.75)
K_Z	Grazing half saturation for Z	mmol N/m^3	1 (0.5–1.2)
m_0	Vertical mixing rate	m/day	0.1 (0.03–0.2)
A_{th}	Concentration at threshold of A	mmol N/m^3	0.1 (0.05–0.15)
r	Plant metabolic loss	1/day	0.05 (0.02–0.07)
r_1	Remineralization rate of D	1/day	0.04 (0.004–0.2)
g	Mortality rate of Z	1/day	0.03 (0.01–0.07)
λ	Mortality rate of F	1/day	0.01 (0.005–0.02)
e	Grazing efficiency for Z	–	0.85 (0.5–1.0)
Q	Maximum growth rate of P	1/day	2 (1–3)
k_1	Light attenuation by water	m	0.1 (0.04–0.12)
k_2	Low light photosynthetic slope	1/langleys	0.04
ϕ	Range for latitude	degree	22.15–23.7
μ	Congestion mortality rate for P	1/day	0.03 (0.02–0.05)
k_P	Congestion half saturation for P	mmol N/m^3	0.75 (0.25–0.75)
p_1	Relative preference for grazing of P	–	0.7 (0.4–0.7)
p_2	Relative preference for gazing of D	–	0.3 (0.25–0.3)
S_0	Solar constant	langleys/min	1.952
a_0	Average albedo of Earth	–	0.3

where B represents any one of the species in system (1)–(5). These equations have two time scales, advection–diffusion terms ($\nabla(\sigma\nabla B) - V\cdot\nabla B$) have a faster time scale that needs a discrete time step of the order of seconds, while reaction terms (biological terms) or source minus sink terms ($f(\alpha, H, B, t)$) have a slow time scale of the order of a day. If the entire system of equations is treated with one time scale, then the biological terms (source terms) of the model become 10^{-2} times smaller than advection–diffusion terms. Thus, the role of biological terms will get neglected if care is not taken. To address stiffness in the system of equations arising due to such time scales differing by several orders of magnitude, operator splitting technique (OST) is used to solve model equations. More details of OST are given in Appendix A.

To integrate the governing system of equations by numerical means, the location (22°20′N, 68°20′E) in Gulf of Kachchh is taken as origin (O) for adopting a rectangular coordinate system. OX and OY are respectively chosen in the zonal and meridional directions of the earth coordinate system. Since the area of the domain of computation is very small, curvature of the earth has been neglected.

Coordinate transformation

To facilitate numerical treatment of discrete analogues of governing equation on an irregular boundary configuration, a coordinate transformation (Figure 6) is introduced, which is based on a new set of independent variables x and ξ, where

$$\xi = \frac{y - b_1(x)}{b_2(x) - b_1(x)}. \tag{19}$$

This mapping transforms the analysis area into a rectangular domain given by $0 \le x \le L_x$, $0 \le \xi \le 1$. Thus, the extremities of the domain $y = b_1(x)$ and $y = b_2(x)$ correspond respectively to $\xi = 0$ and $\xi = 1$. The transformed equations and boundary conditions are given in Appendix B.

Grid generation

(a) The discrete coordinate points for physical plane are defined by

$$x = x_i = i\Delta x \text{ for } i = 0, 1, 2, ..., m;\ \Delta x = \frac{L}{m}, \tag{20}$$

$$y(i) = y_j(i) = j\Delta y(i) \text{ for } j = 0, 1, 2, ..., n,$$

$$\Delta y(i) = \frac{b_2(i) - b_1(i)}{n}, \tag{21}$$

(b) The discrete coordinate points for computational plane are defined by

$$x = x_i = i\Delta x \text{ for } i = 0, 1, 2, 3, 4, ..., m;\ \Delta x = \frac{L}{m}, \tag{22}$$

$$\xi = \xi_j = j\Delta\xi \text{ for } j = 0, 1, 2, 3, 4, ..., n;\ \Delta\xi = \frac{1}{n}. \tag{23}$$

Results and discussion

The present model was found to be sensitive to diffusion coefficient, mortality rate (r, g and λ), half-saturation constants (K_N and K_Z), the mixing rate (m_0), palatability (p_1 and p_2) and additional amount of nutrient entering

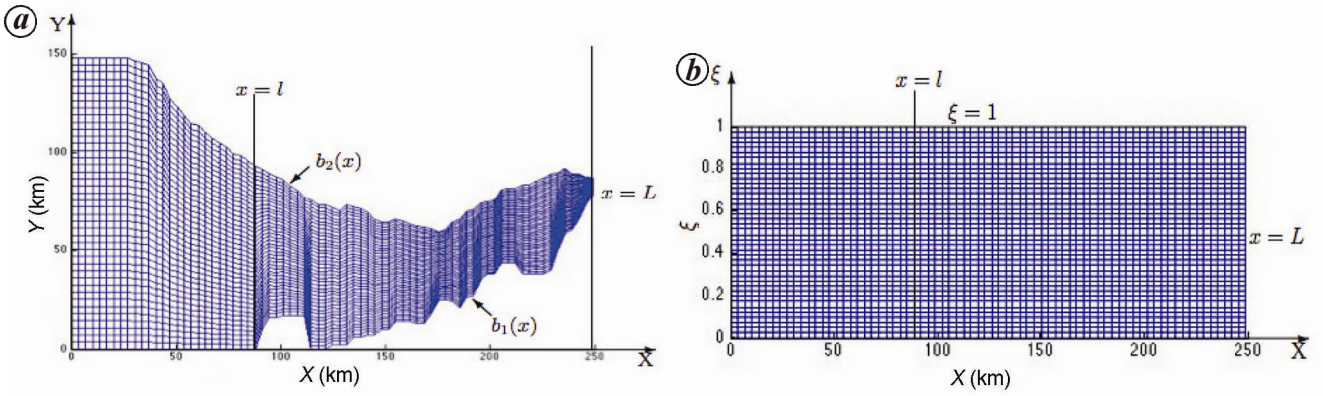

Figure 6. Plot of physical and computational plane. ***a***, Physical plane with variable grid; ***b***, Computational plane with regular grid.

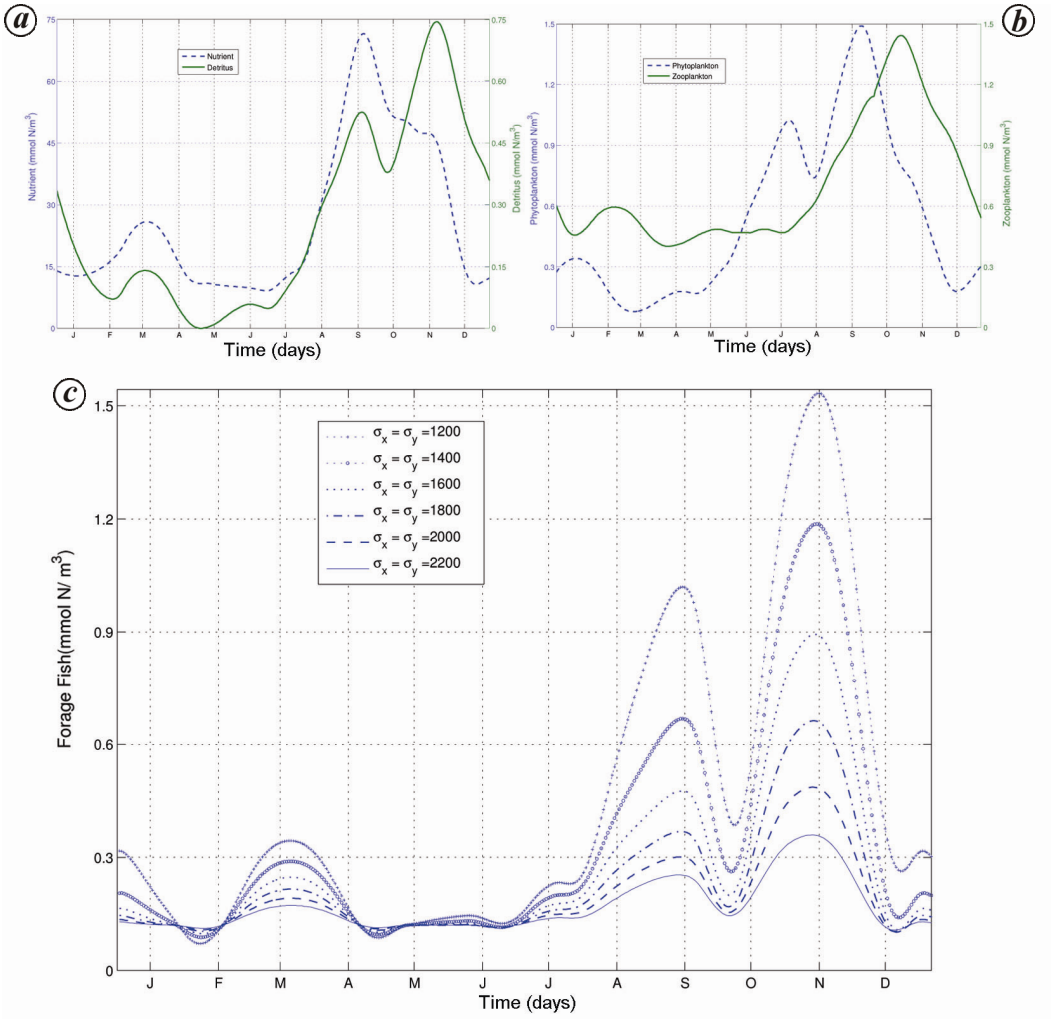

Figure 7. Area-averaged model simulated results. ***a***, Nutrient (- -) and detritus (-); ***b***, Phytoplankton (- -) and zooplankton (-); ***c***, Forage fish.

into the system (N_S). However, model simulated results of forage fish were most sensitive to the diffusion coefficient. All other parameters could be fixed with values taken from literature[2,3,6,15,17]. Their descriptions along with the corresponding ranges are presented in Table 2. Interestingly, change in initial conditions did not have any impact on the profile once the steady state was reached. Such a result was expected because the time-dependent

terms in the equations lose significance as the model simulations approach towards the steady state. Therefore, the present model could be effectively used for ecological modelling of Gulf of Kachchh, though we do not percieve any difficulty in its use for smaller areas of other geographical region. Several model runs were performed to simulate the bimodal oscillation in a year by varying the various parameters given in Table 2 so as to produce this unique feature observed in the available biological and ecological data of Gulf of Kachchh.

The area-averaged concentration of nutrient (Figure 7 *a*) shows a minor peak during spring (March), which again reaches a maximum during post-monsoon (September). Detritus closely follows the same pattern as depicted by the nutrients but with a phase lag of a month. During pre- and post-monsoon, dead bio-products are recycled into nutrients and other organic materials which make the coastal water nutrient rich. However, Figure 7 *b* shows a minor peak during pre-monsoon and a major peak during post-monsoon for both phytoplankton and zooplankton with a time lag of nearly a month. This result is consistent with observed data that also shows a time lag of a month (Figure 2 *c*) between phytoplankton and zooplankton. During pre- and post-monsoon, the region is rich in phytoplankton concentration because of high nutrients and sufficient light available for its growth. This condition leads to larger zooplankton population in the area, since they feed on phytoplankton. Area-averaged concentration of forage fish (Figure 7 *c*) is higher during March (minor peak) and September and November (major peak). These periods are favourable for forage because of food abundance. Forage fish population is observed to be maximum during the same period (pre- and post-monsoon) of maximum phytoplankton and zoo-plankton. The concentration decreases during March–May and July–September due to less planktons and forage fish become prey themselves. As mentioned earlier, the distribution of forage fish is seen to be sensitive to the change in values of the diffusion coefficient. The concentrations of forage fish decrease as diffusion coefficient increases, though decrease rate is maximum during the peak forage distribution period (Figure 7 *c*).

The biological model without advection–diffusion terms could reproduce only one peak in a year in the absence of ocean currents (Figure 8). However, the situation changed dramatically when ocean currents were incorporated in the simulations and two peaks are observed in a year (Figure 7). This result also underscores the significance of dynamics on the ecological changes in the region as oceanic physical processes have major role during marine biological processes. The spatio-temporal model in this study appears to be quite suitable for the ecological modelling of Gulf of Kachchh as it can reproduce the influence of periodic pattern of ocean currents on the pattern of ecological dynamics.

Figure 9 *a–c* compares the trends of model simulated results with observed data. Chlorophyll and phytoplankton are two different quantities but chlorophyll is directly proportional to phytoplankton. Therefore, seasonal pattern of chlorophyll and plankton should be similar. A comparison of simulated phytoplankton concentration and SeaWiFs derived monthly mean chlorophyll *a* is shown in Figure 9 *a* while Figure 9 *b* presents its direct evaluation with *in situ* data[12]. The large number of cells consist maximum biomass of plankton and similar patterns. SeaWiFs derived monthly mean chlorophyll shows two minor peaks in January–February and April but the major peak could be noticed in September. *In situ* data shows two minor peaks in January and May–June and one major peak in September. Model simulated phytoplankton also shows one minor and one major peak in the same period showing a marginal shift from *in situ* data (Figure 9 *b*). However, simulated zooplankton is also compared with the *in situ* data[12]. *In situ* data shows one minor peak in March and one major peak in October. Similarly, model-simulated zooplankton also shows one minor and major peak in the same period with marginal shift from *in situ* data (Figure 9 *c*). The qualitative comparison of model simulated results and observed data show similar pattern.

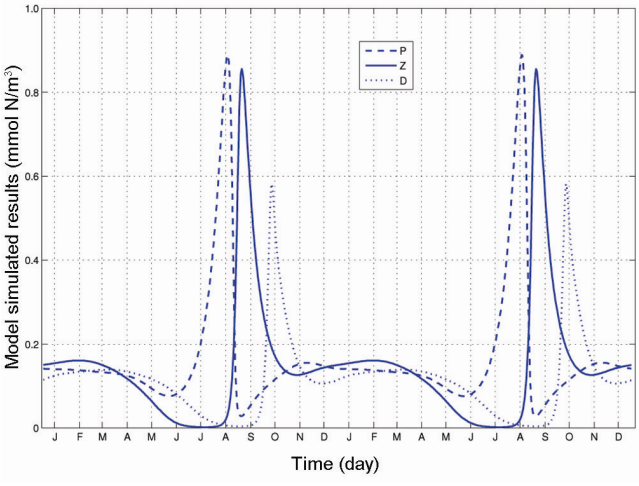

Figure 8. Model simulated results without advection–diffusion.

Conclusion

The ecological model used in this study reproduces the variations in concentration of different species that match with observations during the period in which their concentration peaks. The results, like those of other models, depend heavily on parameter values used in the governing equations. Non-linear oscillations or distinct seasonal patterns and periodicity found in phytoplankton, zooplankton and forage fish distribution usually correlate well with changes in environmental parameters, particularly light, nutrient availability and factors like palatability associated with grazing[15].

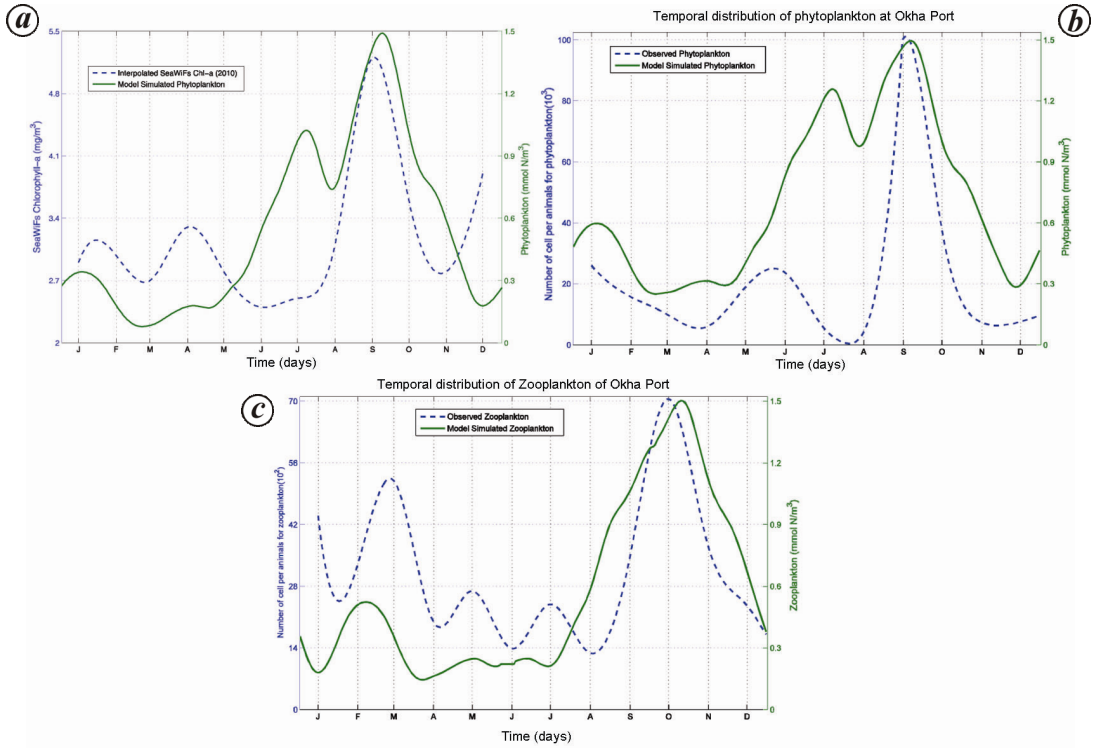

Figure 9. Plot of observed and model simulated data. ***a***, Area-averaged SeaWiFs Chl *a* and model simulated phytoplankton; ***b***, *In situ* and model simulated phytoplankton at Okha port. ***c***, Observed (- -) and model simulated zooplankton (-) at Okha port.

The present study brings out a successful approach based on a mathematical model to exploit the limited data resources now available to carry out intense research in this area. According to model simulated results as shown in Figures 7 and 8, the oceanic circulations play an important role during biological processes and redistribution of marine plankton and forage fish. The model is able to reproduce the trend in observed/satellite data as shown in Figure 9. The photosynthesis rate of phytoplankton and physical processes are responsible for reproducing bimodal oscillation, periodic behaviour and spatio-temporal distribution of biological productivity.

The coordinate transformation is useful to convert irregular boundary domain into required rectangular domain during numerical simulations for higher order of accuracy. Biological processes are very slow compared to physical processes. Thus it takes days to observe changes in the marine plankton and forage fish whereas changes in ocean circulations and other physical processes can be observed within seconds or minutes. OST helps in better handling of slow and fast time scales together. The model is highly promising and there is a need to include more species and recent data for better validation.

Appendix A. Operator splitting technique (OST)

In operator splitting method, the operator $(\partial B/\partial t)$ is split into two parts corresponding to the two different time scales[20]. The equations are handled in the following way:

1. Advection–diffusion equation with temporal scale in seconds.

$$\frac{\partial B}{\partial t} = \nabla(\sigma \nabla B) - V \nabla B. \tag{A1}$$

2. Ecological equation with temporal scale in days.

$$\frac{\partial B}{\partial t} = f(\alpha, M, B, t). \tag{A2}$$

Global temporal step size for advection–diffusion-reaction equation is Δt. Local temporal step size for advection–diffusion term (physical or transport term) is Δt_1 and that for reaction term (biological or source term) is Δt_2.

Method of solution

1. Solution of equation (18) for $(0 \le t \le \Delta t)$:

(i) Equation (A1) solved for the following initial and boundary conditions: Initial condition: $B(x, y, 0) = B_0(x, y)$ and boundary conditions $(\partial B/\partial \eta) = 0$ at coastal boundary and $B(x, y, t) = B_b$ at open ocean.

Solution of eq. (A1) at $t = \Delta t$ using finite difference scheme (Crank–Nicolson method) with step size Δt_1 is obtained as

$$B(x, y, \Delta t) = B_1^P(x, y). \tag{A3}$$

Table A1. Initial and boundary parameters

Parameter	Parameter description	Unit	Values
N_0	Nutrient at initialization time of model	mMol/m^3	1
N_b	Nutrient at boundary	mMol/m^3	0.01–0.9
P_0	Phytoplankton at initialization time of model	mMol/m^3	0.2
P_b	Phytoplankton at boundary	mMol/m^3	0.01–0.6
Z_0	Zooplankton at initialization time of model	mMol/m^3	0.2
Z_b	Zooplankton at boundary	mMol/m^3	0.01–0.6
D_0	Detritus at initialization time of model	mMol/m^3	0.1
D_b	Detritus at boundary	mMol/m^3	0.01–0.3
F_0	Forage fish at initialization time of model	mMol/m^3	0.2
F_b	Forage fish at boundary	mMol/m^3	0.01–0.6
Δt	Combination time step of two processes	day	1
Δt_1	Time step for physical processes	Second	86.4
Δt_2	Time step for biological processes	day	0.001
Δx	Spatial step along zonal direction	m	5565.9
Δy	Spatial step along meridional direction	m	347.83–5565.9

(ii) Equation (A2) solved for the following initial conditions:

Initial condition: $B(x, y, 0) = B_1^P(x, y)$.

Solution of eq. (A2) at $t = \Delta t$ using Runge–Kutta method with step size Δt_2 is obtained as

$$B(x, y, \Delta t) = B_1^B(x, y). \tag{A4}$$

Solution of eq. (18) at $t = \Delta t$ is

$$B(x, y, t = \Delta t) = B_1^B(x, y). \tag{A5}$$

2. Solution of eq. (18) for $(n - 1)\Delta t \le t \le n\Delta t$:

(i) Equation (A1) solved for the following initial and boundary conditions:

Initial condition: $B(x, y, 0) = B_{n-1}^B(x, y)$ and boundary conditions: $\partial B/\partial \eta = 0$ at coastal boundary and $B(x, y, t) = B_b$ at open ocean.

Solution of eq. (A1) at $t = n\Delta t$ using finite difference scheme (Crank–Nicolson method) taking step size Δt_1 is obtained as

$$B(x, y, n\Delta t) = B_n^P(x, y). \tag{A6}$$

(ii) Equation (A2) solved for the following initial conditions:

Initial condition: $B(x, y, 0) = B_n^P(x, y)$.

Solution of eq. (A2) at t = $n\Delta t$ using Runge–Kutta method taking step size Δt_2 is obtained as

$$B(x, y, n\Delta t) = B_n^B(x, y). \tag{A7}$$

Solution of eq. (18) at $t = n\Delta t$ is

$$t = n\Delta t \text{ is } B(x, y, t = n\Delta t) = B_n^B(x, y),\ n = 1, 2, ... \tag{A8}$$

Appendix B. Transformed equations and boundary conditions

(a) After the coordinate transformation, eqs (1–5) are in the form

$$\frac{\partial B}{\partial t} + u\frac{\partial B}{\partial x} + V_\xi \frac{\partial B}{\partial \xi} = \sigma \frac{\partial^2 B}{\partial x^2} + \Lambda_\xi \frac{\partial^2 B}{\partial \xi^2} + \Lambda_{x\xi} \frac{\partial^2 B}{\partial x \partial \xi} + f(B, H, t), \tag{B1}$$

$$V_\xi = \frac{1}{b}\left\{v - \left(u + \frac{2\sigma}{b}\frac{\partial b}{\partial x}\right)\left(\frac{\partial b_1}{\partial x} + \xi\frac{\partial b}{\partial x}\right)\right\} + \frac{\sigma}{b}\left(\frac{\partial^2 b_1}{\partial x^2} + \xi\frac{\partial^2 b}{\partial x^2}\right). \tag{B2}$$

$$\Lambda_\xi = \frac{\sigma}{b^2}\left\{1 + \left(\frac{\partial b_1}{\partial x} + \xi\frac{\partial b}{\partial x}\right)^2\right\}, \quad \Lambda_{x\xi} = -\frac{2\sigma}{b}\left(\frac{\partial b_1}{\partial x} + \xi\frac{\partial b}{\partial x}\right), \tag{B3}$$

where $f(B, H, t)$ is the biological term corresponding to N, P, Z, D and F.

(b) Boundary conditions

$B(x, 0, t) = B_0(x, t)$ for $0 \le x < l$ and

$$\frac{\partial B}{\partial \xi} = 0 \text{ for } l \le x \le L \text{ at } \xi = 0, \tag{B4}$$

$$B(0,\xi,t) = B_0(\xi,t) \text{ for } 0 \le \xi \le 1 \text{ at } x = 0, \quad \text{(B5)}$$

$$\frac{\partial B}{\partial \xi} = 0 \text{ for } 0 \le x \le L \text{ at } \xi = 1, \quad \text{(B6)}$$

$$\frac{\partial B}{\partial \xi} = 0 \text{ for } 0 \le \xi \le 1 \text{ at } x = L. \quad \text{(B7)}$$

1. Kumari, B., Raman, M. and Mali, K., Locating tuna forage ground through satellite remote sensing. *Int. J. Remote Sens.*, 2009, **30**(22), 5977–5988.
2. Evans, G. T. and Parslow, J. S., A model of annual Plankton cycles. *Biol. Oceanogr*., 1985, **3**, 327-347.
3. Fasham, M. J. R., Ducklow, H. W. and Mckelvie, S. M., A nitrogen-based model of plankton dynamics in the oceanic mixed layer. *J. Mar. Res*., 1990, **48**, 591–639.
4. Edwards, A. M., Adding detritus to a nutrient–phytoplankton–zooplankton model: a dynamical – systems approach. *J. Plankton Res*., 2001, **23**(4), 389–413.
5. Lehodey, P., The pelagic ecosystem of tropical Pacific Ocean: dynamic spatial modelling and biological consequences of ENSO. *Prog. Oceanogr.*, 2001, **49**, 439–468.
6. Lehodey, P. *et al.*, Predicting skipjack forage distributions in the equatorial Pacific using a coupled dynamical bio-geochemical model. *Fish. Oceanogr*., 1998, **7**, 317–325.
7. Mohanty, R. K., An operator splitting method for an unconditionally stable difference scheme for a linear hyperbolic equation with variable coefficients in two space dimensions. *Appl. Math. Comput.*, 2004, **152**, 799–806.
8. Khan, L. A. and Liu, P. L. F., An operator splitting algorithm for coupled one-dimensional advection–diffusion–reactions equations. *Comput. Methods Appl. Mech. Eng*., 1995, **127**, 181–201.
9. Wheeler, M. F. and Dawson, C. N., An operator-splitting method for advection–diffusion-reaction problems. Technical report 87-9, Mathematical Sciences Department, Rice University, Houston, Texas, 1987.
10. Kunte, P. D., Wagle, B. G. and Sugimori, Y., Sediment transport and depth variation study of the Gulf of Kutch using remote sensing. *Int. J. Remote Sens*., 2003, **24**(11), 2253–2263.
11. Shirodhkar, P. V., Pradhan, U. K., Fernandes, D., Haldankar, S. R. and Rao, G. S., Influence of anthropogenic activities on the existing environmental conditions of Kandla Creek (Gulf of Kutch). *Curr. Sci.*, 2010, **98**(6), 815–828.
12. Bhaskaran, M. and Gopalakrishnan, P., Observations on the marine plankton in the Gulf of Kutch, off Port Okha. *Indian J. Fish*., 1971, **18**(1&2), 99–108.
13. Shankar, D., Vinayachandran, P. N. and Unnikrishnan, A. S., The monsoon currents in the North Indian Ocean. *Prog. Oceanogr.*, 2002, **52**, 63–120.
14. Steel, J. H., Plant production in the northern North Sea, Scottish Home Department. Marine research report No. 7. HMSO, Edinburgh, 1958.
15. Dube, A., Jayaraman, G. and Rani, R., Modelling the effects of variable salinity on the temporal distribution of plankton in shallow coastal lagoons. *J. Hydro-Environ. Res*., 2010, **4**(3), 199–209.
16. Rani, R. and Jayaraman, G., A minimal model for Plankton dynamics in shallow coastal lagoons – Chilika lagoon, a case study. *Int. J. Emerging Multidiscipl. Fluid Sci.*, 2010, **2**(2–3), 123–141.
17. Ishizaka, J., Coupling of coastal zone color scanner data to a physical–biological model of the Southeastern US continental shelf ecosystem, 2, An Eulerian Model. *J. Geophys. Res*., 1990, **95**(C11), 20201–20212.
18. Chauhan, O. S., Jayakumar, S., Menezes, A. A. A., Rajawat, A. S. and Nayak, S. R., Anomalous inland influx of the River Indus, Gulf of Kachchh, India. *Marine Geol*., 2006, **229**(1), 91–100.
19. Chu, P. C., Ivanov, L. M. and Margolina, T. M., On non-linear sensitivity of marine biological model to parameter variations. *Ecol. Modell*., 2007, **206**, 369–382.
20. Kumar, V. and Jayaraman, G., Operator splitting technique in biological oceanography – Central Arabian Sea, A Case Study. In Proceedings of Fluid Mechanics and Fluid Power, Society of IIT Bombay, 2012, pp. 225-1–225-7, ISBN 978-81-925-494-0-8.

ACKNOWLEDGEMENTS. The work done in the present paper was partially funded by Space Applications Centre, ISRO, Government of India. The authors thank scientists at MBD, SAC, ISRO and Prof. O. P. Sharma (CAS, IIT Delhi) for their suggestions. V.K. is thankful to CSIR for providing scholarship.

Received 2 November 2014; revised accepted 21 April 2017

doi: 10.18520/cs/v113/i06/1107-1119